Available online at www.sciencedirect.com
ScienceDirect
Journal of Crystal Growth 310 (2008) 1546–1551
JOURNAL OF CRYSTAL GROWTH
www.elsevier.com/locate/jcrysgro

Influence of acoustic streaming on the stability of melt flows in horizontal Bridgman configurations

W. Dridi*, D. Henry, H. Ben Hadid

Laboratoire de Mécanique des Fluides et d'Acoustique, CNRS/Université de Lyon, Ecole Centrale de Lyon/Université Lyon 1/INSA de Lyon, ECL, 36 Avenue Guy de Collongue, 69134 Ecully Cedex, France

Available online 12 November 2007

Abstract

We study the effect of acoustic streaming (steady flow generated by progressive acoustic waves) on the stability of convective flows associated with crystal growth from melt in horizontal Bridgman configurations. We consider two simple configurations: an extended fluid layer submitted to a horizontal temperature gradient and a laterally heated parallelepipedic cavity. In both cases, the dependence of the critical Grashof number Gr_c on the acoustic intensity (monitored through the acoustic parameter A) is determined for given values of the Prandlt number and of the dimension of the acoustic source H_b. In the case of the extended fluid layer, it is shown that for rather small beam widths H_b, the acoustic streaming destabilizes the buoyant flows, but for a large beam width, a range of acoustic intensities A is found for which the buoyant flows are stabilized. An adequate decentring of the beam can also enhance the stabilization. In the case of the parallelepipedic cavity, the numerical calculations for a quite large beam width have shown that the critical thresholds for the two first (steady, and then oscillatory) bifurcations clearly increase when the acoustic streaming contribution is enhanced.

PACS: 47.20.Bp; 47.20.Ky; 43.25.Nm

Keywords: A1. Computer simulation; A1. Convection; A2. Bridgman technique; A2. Growth from melt

1. Introduction

Directional solidification of metallic alloys or semiconductors is often accompanied by oscillatory flows in the melt-phase which affect the crystal quality by creating undesirable striations. To enhance the crystal quality in the horizontal Bridgman configurations, we propose to apply progressive acoustic waves of high frequency in the bulk of the melt. The experimental results of Kozhemyakin [1] showed that the use of ultrasonic vibrations can attenuate and even sometimes eliminate the striations. Moreover, it is well known that by applying ultrasonic waves in the bulk of a fluid, a steady flow called Eckart streaming is generated [2–6]. It is a nonlinear effect which owes its origin to the action of Reynolds stresses and the dissipation of acoustic energy flux. In the Eckart streaming, the flow generated inside the ultrasound beam, moves away from the source within the body of fluid. This streaming flow can alter the structure of the buoyant flow and modify its stability properties. It is this point we want to study in the paper for two simple configurations, an extended fluid layer and a parallelepipedic cavity.

The flow velocities due to both acoustic streaming and convection are known analytically in the case of the laterally heated extended fluid layer [7], and they have been determined numerically in the case of the side heated three-dimensional cavity. The linear stability of these solutions has then been studied. For the extended layer, we present the variation of the critical Grashof number Gr_c as a function of the Prandlt number Pr and the way these thresholds are affected by the acoustic streaming for a fixed acoustic beam width ($H_b = 0.8$). We then focus on the neutral stability curves for the two-dimensional stationary instabilities which prevail at small Pr, and determine the thresholds as a function of the acoustic streaming intensity at a fixed value of Pr ($Pr = 0.01$), for different values of H_b

*Corresponding author.
E-mail address: dridiwalid@gmail.com (W. Dridi).

0022-0248/$ - see front matter © 2007 Elsevier B.V. All rights reserved.
doi:10.1016/j.jcrysgro.2007.11.014

and a centered or non-centered beam. For a parallelepipedic cavity with aspect ratios $A_x = \text{length/height} = 4$ and $A_y = \text{width/height} = 1$ and at $Pr = 0.01$, the bifurcation diagrams related to the convective flows, with and without the influence of acoustic streaming, have been determined. They show a strong influence of the acoustic streaming on the stationary and oscillatory thresholds.

2. Formulation of the problem and numerical techniques

2.1. Formulation of the problem

We consider an incompressible Newtonian fluid layer of height h, heated laterally (applied horizontal temperature gradient $\nabla\bar{T}$) and subject to a constant radiation pressure caused by an ultrasonic beam, with a normalized width $H_b = \text{height of acoustic source/height of fluid layer}$, applied in the positive x direction. The fluid is assumed to have constant physical properties (kinematic viscosity ν, thermal diffusivity κ, density ρ), except that, according to the Boussinesq approximation, the fluid density is considered as temperature dependent in the buoyancy term with a linear law $\rho = \rho_0(1 - \beta(\bar{T} - \bar{T}_0))$, where β is the thermal expansion coefficient, $\bar{T}_0$ is a reference temperature, and ρ_0 is the value of the density at $\bar{T}_0$. The ultrasound field is assumed to be an attenuated plane wave traveling in the positive x direction. The attenuation of the acoustic wave in the viscous fluid, due to the dissipation of acoustic energy flux, generates a body force $\boldsymbol{F}$ acting within the ultrasound beam and equal to the spatial variation of the Reynolds stress [2,5]. The components of $\boldsymbol{F}$ are given by Lighthill [2] as $F_j = -\partial(\overline{\rho u_i' u_j'})/\partial x_i$, where i and j denote the three directions of space, x_i is the spatial coordinate in the i direction, the u_i' are the fluctuating velocities in the sound wave and the bar signifies a mean value in time. The equivalent vector expression of $\boldsymbol{F}$, which can be found for example in Nyborg [5] and Frampton et al. [6], is $\boldsymbol{F} = -\rho(\overline{(\boldsymbol{u}'\cdot\nabla)\boldsymbol{u}' + \boldsymbol{u}'(\nabla\cdot\boldsymbol{u}')})$. For a plane wave traveling in the positive x direction, the particle velocity in the ultrasound beam can be written as $u_1' = V_a\,e^{-\alpha x}\sin(\omega t - kx)$, where ω, k, V_a and α are the angular frequency, the wave number, the particle velocity amplitude and the spatial attenuation factor of the sound wave, respectively. The force $\boldsymbol{F}$ is therefore oriented along the x-axis and its intensity is given by $F = \rho\alpha V_a^2\,e^{-\alpha x}$ [5]. Now, provided the beam is only slightly divergent and the attenuation of the wave sufficiently weak, a body force which is constant ($F = \rho\alpha V_a^2$) inside the section of the acoustic beam and zero everywhere else in the cavity, can be defined. This body force is introduced in the Navier–Stokes equations [2] which, in our case, are coupled with an energy equation through the buoyancy term. Using h, h^2/ν, ν/h, $\rho\nu^2/h^2$ and $\gamma = \nabla\bar{T}h$ as scales for length, time, velocity, pressure and temperature, respectively, these equations take the following form:

$$\nabla\cdot\boldsymbol{V} = 0, \tag{1}$$

$$\frac{\partial\boldsymbol{V}}{\partial t} + (\boldsymbol{V}\cdot\nabla)\boldsymbol{V} = -\nabla P + \nabla^2\boldsymbol{V} + GrT\boldsymbol{e}_z + A\delta_b\boldsymbol{e}_x, \tag{2}$$

$$\frac{\partial T}{\partial t} + (\boldsymbol{V}\cdot\nabla T) = \frac{1}{Pr}\nabla^2 T. \tag{3}$$

In both configurations, we have no slip conditions ($\boldsymbol{V} = 0$) and insulating thermal boundary conditions on all boundaries. The dimensionless variables are the velocity vector $\boldsymbol{V} = (u, v, w)$, the pressure P and the temperature $T = (\bar{T} - \bar{T}_0)/\gamma$, and $\boldsymbol{e_z}$ and $\boldsymbol{e_x}$ are the unit vectors in the vertical and longitudinal directions, respectively. The nondimensional parameters are the Grashof number, $Gr = \beta g\gamma h^3/\nu^2$, the Prandtl number, $Pr = \nu/\kappa$, and the acoustic parameter $A = \alpha V_a^2 h^3/\nu^2$ which is the dimensionless expression of the acoustic force $\boldsymbol{F}\cdot\delta_b$ is a function of the space coordinates and its value is 1 inside the ultrasound beam and 0 outside.

2.2. Numerical techniques

The extended layer is considered as infinite in both longitudinal x and transverse y directions, and a stationary parallel flow solution only depending on the vertical coordinate z can be found [7]. The stability of the basic flow is then investigated by a temporal linear analysis. The perturbations verify a linear system of equations which after the expansion of the perturbations as normal modes $((\boldsymbol{v}, p, \theta) = (\boldsymbol{v}, p, \theta)(z)e^{i(k_x x + k_y y) + st})$ leads to an eigenvalue problem solved by a spectral Tau Chebyshev method. k_x and k_y are real wave numbers in the longitudinal x and transverse y directions, respectively, and $s = s_r + i\omega$ is a complex eigenvalue whose real part represents an amplification rate and imaginary part an oscillation frequency.

For the three-dimensional cavity, the governing equations are solved using a spectral element method [8]. The time discretization is carried out using a semi-implicit splitting scheme. A continuation technique based on a Newton solver is implemented, which allows both steady state solving and calculation of bifurcation points [8]. The way to implement the Newton solver using time iterations follows the original ideas of Mamun and Tuckerman [9].

3. Results

3.1. Extended layer results

The first results presented in Fig. 1 concern the effect of acoustic streaming on the different instabilities appearing for a Prandtl number between 10^{-3} and 0.4, i.e., the two-dimensional stationary instabilities (transverse rolls) which dominate for small Pr values, and the three-dimensional oscillatory and stationary instabilities (longitudinal rolls) which successively prevail when Pr is further increased. An acoustic beam of normalized width $H_b = 0.8$ is considered, with two intensities corresponding to $A = 5\times10^4$ and 10^5. The two-dimensional instabilities become oscillatory when

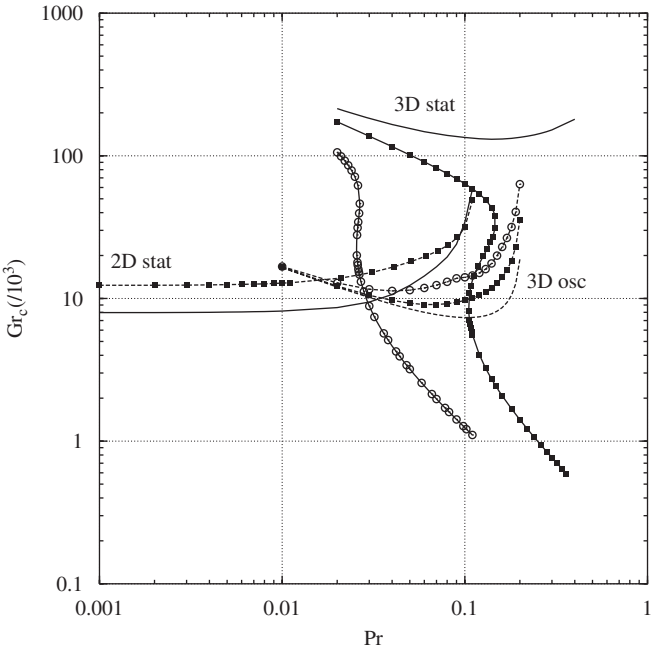

Fig. 1. Variation of the thresholds Gr_c as a function of Pr for 2D stationary, 3D stationary, and 3D oscillatory instabilities (so called from their properties at $A=0$) for different values of A ($A=0$ (thick curves without symbols), $A=5\times10^4$ (black squares), and $A=10^5$ (circles)) ($H_b=0.8$). The solid curves denote stationary thresholds and the dashed curves oscillatory thresholds.

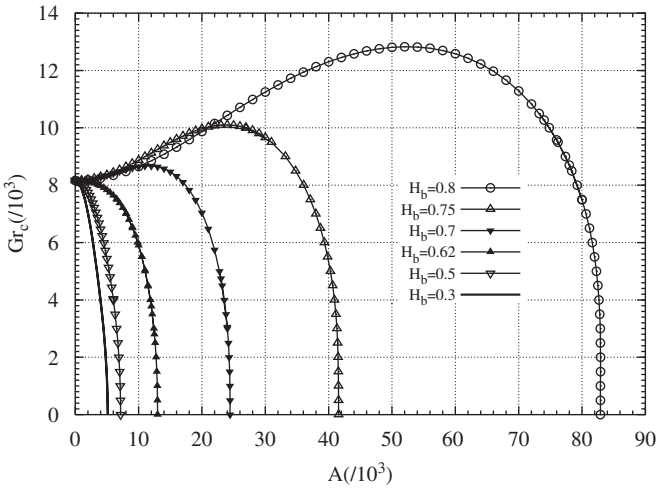

Fig. 2. Variation of the thresholds Gr_c as a function of A for the 2D stationary instabilities for different values of H_b and $Pr=0.01$.

the acoustic beam is applied, and the thresholds, which increase for $A=5\times10^4$, then disappear for $A=10^5$ as this value is above the critical threshold $A_c=82\,647$ for pure acoustic streaming [7]. Concerning the three-dimensional instabilities, the two types of instabilities evolve differently when the acoustic beam is applied. The thresholds of the stationary instabilities strongly decrease while those of the oscillatory instabilities increase.

We give now precisions on the action of the ultrasonic beam on the two-dimensional stationary instabilities which prevail at small values of Pr. The results which have been obtained for $Pr=0.01$ are shown in Fig. 2. The neutral stability curves give the evolution of the thresholds Gr_c with the acoustic intensity A for different values of the beam width H_b. For $A=0$, the pure thermal threshold is obtained. From Fig. 2, we see that for values of H_b lower than 0.6, the ultrasound waves cause a strong decrease of Gr_c, thus contributing to destabilize the basic flow. For higher values of H_b, the value of Gr_c first increases, then reaches a maximum and finally strongly decreases. A range of A values in which the convective flow is stabilized by the ultrasound waves is thus determined in this case. In any case, the curves eventually cut the $Gr=0$ axis at a value of A corresponding to the critical acoustic intensity for the onset of instabilities in an isothermal fluid layer [7]. All these two-dimensional instabilities are oscillatory (except at $A=0$) and they are connected to the shear zones appearing in the basic flow profiles. These shear zones are located in the center of the layer for the thermal case without acoustic streaming and at the boundaries of the acoustic beam for pure acoustic streaming. In mixed situations, they are disposed in a more complex manner.

We finally consider non-centered beams and look to their effects on the onset of the two-dimensional stationary instabilities. The characteristics of the beam are now its width H_b and the position of its center z_c ($-0.5\leqslant z_c\leqslant0.5$). We choose a constant beam width, $H_b=0.3$, and two opposite positions of the beam, $P_1(z_c=0.1)$ and $P_2(z_c=-0.1)$, corresponding, respectively, to an acoustic streaming flow opposing and reinforcing the convective flow. The results are presented in Fig. 3 with the neutral stability curves (Gr_c as a function of A) which are compared to that obtained when the beam is centered (position $C(z_c=0)$). We see that for the position P_1 of the beam, a strong stabilizing influence can be obtained by acoustic streaming, in a situation where the convective flow was destabilized when the beam was centered. In the contrary, for the opposite position P_2 of the beam, a destabilizing influence of the acoustic streaming, stronger than in the centered case, is observed. From these results, it seems that it could be interesting to use non-centered beams to enhance the stabilizing influence of acoustic streaming, but the beam has to be in a position at which acoustic streaming opposes the convective flow. Note that the neutral curves obtained for the two opposite positions P_1 and P_2 of the beam intersect the $Gr=0$ axis at the same value of A. This can be understood from Fig. 4 where the critical thresholds A_c for the isothermal fluid layer are given as a function of the position of the beam center, for a given beam width $H_b=0.3$. Indeed, we see that for opposite positions of the beam, the same thresholds A_c are obtained. This is due to the fact that the flows obtained are symmetric one of the other with respect to the center of the layer, and thus completely equivalent. Fig. 4 also shows that for $H_b=0.3$, the thresholds A_c first decrease when the beam is moved away from the center, until the positions $|z_c=0.2|$ beyond which the thresholds increase.

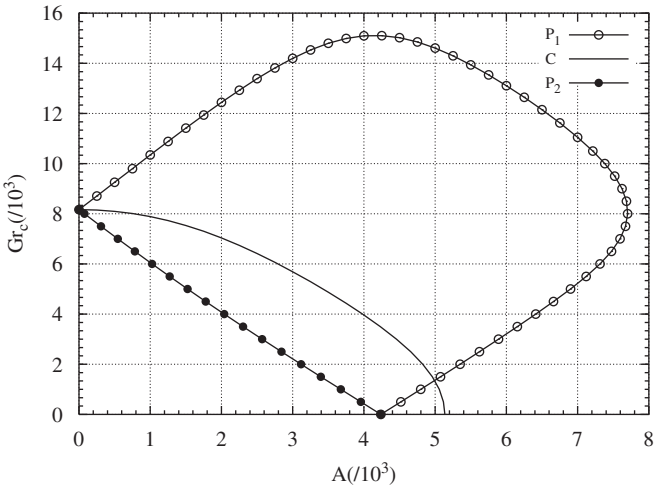

Fig. 3. Variation of the thresholds Gr_c as a function of A for the 2D stationary instabilities for $Pr = 0.01$, $H_b = 0.3$ and different positions of the beam, $P_1(z_c = 0.1)$, $C(z_c = 0)$, and $P_2(z_c = -0.1)$.

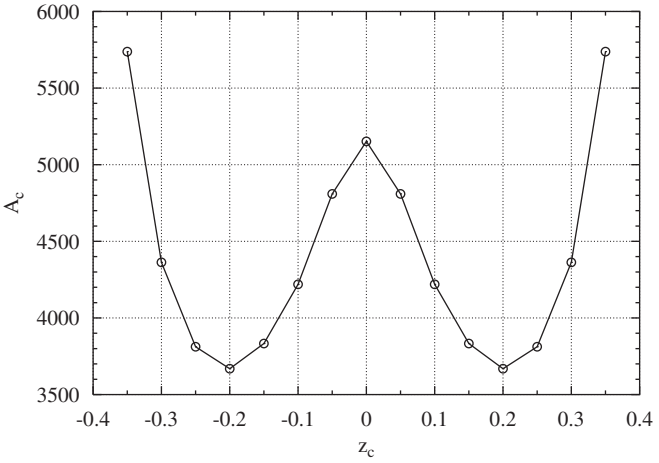

Fig. 4. Variation of the thresholds A_c as a function of the position of the center of the acoustic source z_c for the 2D oscillatory instabilities in an isothermal fluid layer for $H_b = 0.3$.

3.2. Three-dimensional cavity results

The schematic diagram of the geometry of the three-dimensional cavity is given in Fig. 5. It allows to see the principal axes and planes of the cavity, which will be useful to describe the symmetry properties of the flows. We recall that the cavity has a square cross-section ($A_y =$ width/height $= 1$) and that its normalized length is 4 ($A_x =$ length/height $= 4$).

For the laterally heated three-dimensional cavity, we have first calculated the flows without acoustic streaming and established a bifurcation diagram giving the evolution of the flow as a function of the Grashof number Gr. This bifurcation diagram is presented in Fig. 6. On the basic branch (which evolves continuously from the small values of Gr), the solution presents a reflection symmetry S_l with respect to the longitudinal vertical V_1 plane, and a π-

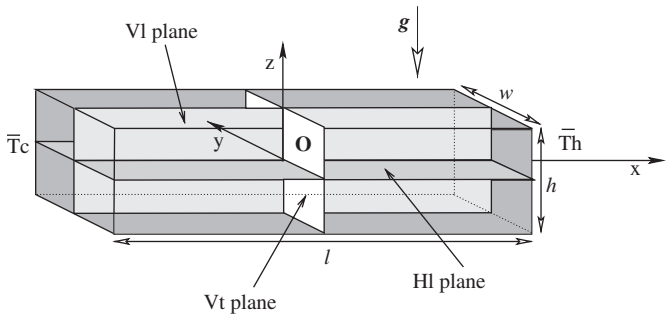

Fig. 5. Schematic diagram of the 3D cavity.

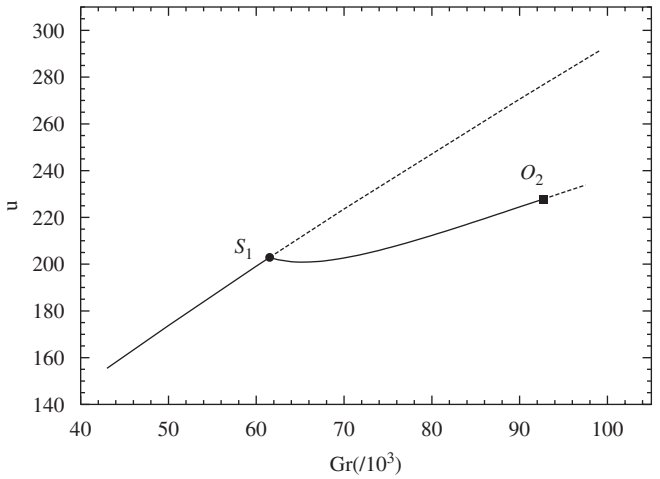

Fig. 6. Bifurcation diagram for a laterally heated cavity ($A_x = 4$, $A_y = 1$, $Pr = 0.01$) without acoustic streaming. S_1 is a steady threshold and O_2 an oscillatory threshold.

rotational symmetry S_r about the transverse y-axis (Fig. 7(a)). The combination of these two symmetries gives a symmetry S_c with respect to the center point O of the cavity. The first bifurcation S_1 on this branch is found for $Gr_c = 61\,530$. It is a supercritical pitchfork bifurcation which breaks both S_l and S_r symmetries (see the eigenvector in Fig. 7(a1) which is antisymmetric with respect to these both symmetries). The steady bifurcated solution which only keeps the symmetry S_c with respect to the center point of the cavity (Fig. 7(b)) becomes then unstable at a Hopf bifurcation point O_2 for $Gr_c = 92\,696$. The oscillatory flow which is triggered at this point keeps the central symmetry, as can be seen from the symmetry of the critical complex eigenvector given in Figs. 7(b1) and (b2).

The laterally heated cavity is now submitted to an acoustic beam generated by an ultrasound source which is supposed to be square and of dimensionless size $H_b = 0.62$. Under the influence of this acoustic beam (of fixed intensity $A = 40\,000$), the flow solutions are changed and a new diagram of bifurcation is obtained (Fig. 8). The solution on the basic branch now only presents a reflection symmetry S_l with respect to the V_1 plane (Fig. 9(a)). The first bifurcation S_1, which occurs at $Gr_c = 81\,540$, is a supercritical pitchfork bifurcation which breaks the S_l symmetry (see the eigenvector in Fig. 9(a1) which is antisymmetric

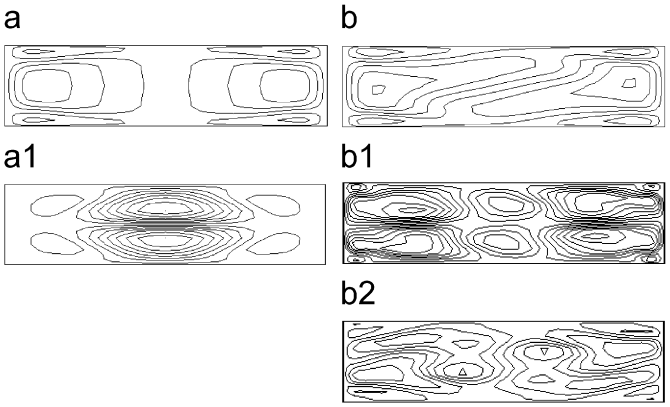

Fig. 7. Laterally heated cavity without acoustic streaming: structure of the flow on the basic branch at S_1 (a) and on the bifurcated branch at O_2 (b). Structure of the critical eigenvector at the steady bifurcation S_1 (a1) and at the Hopf bifurcation O_2 (real part (b1) and imaginary part (b2)). The plot give isovalues of the longitudinal velocity u in the H_1 plane.

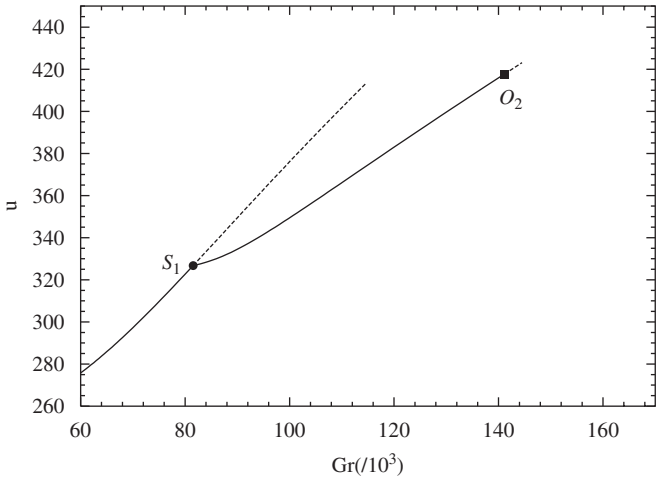

Fig. 8. Bifurcation diagram for a laterally heated cavity ($A_x = 4$, $A_y = 1$, $Pr = 0.01$) with acoustic streaming ($A = 40\,000$). S_1 is a steady threshold and O_2 an oscillatory threshold.

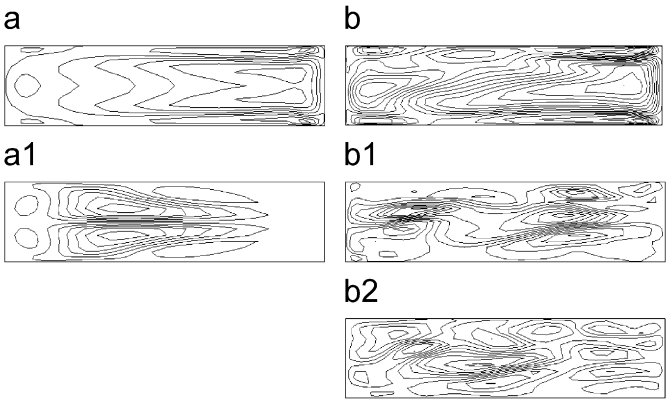

Fig. 9. Laterally heated cavity with acoustic streaming ($A = 40\,000$): structure of the flow on the basic branch at S_1 (a) and on the bifurcated branch at O_2 (b). Structure of the critical eigenvector at the steady bifurcation S_1 (a1) and at the Hopf bifurcation O_2 (real part (b1) and imaginary part (b2)). The plots give isovalues of the longitudinal velocity u in the H_1 plane.

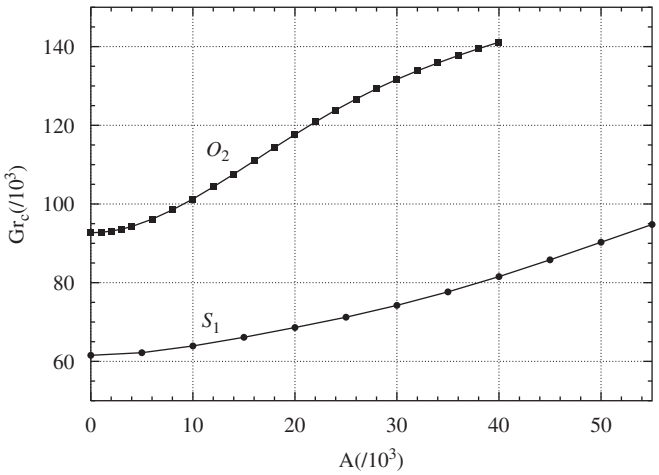

Fig. 10. Stationary threshold, S_1, on the basic branch of solutions, and oscillatory threshold, O_2, on the bifurcated branch, as a function of A ($A_x = 4$, $A_y = 1$, $Pr = 0.01$, $H_b = 0.62$).

with respect to this symmetry). The steady bifurcated solution has no more symmetries (Fig. 9(b)), and it becomes unstable at a Hopf bifurcation point O_2 for $Gr_c = 141\,119$. The complex eigenvector at this point (Figs. 9(b1) and (b2)) has also no more symmetries, as well as the oscillatory flow which is triggered beyond this point. By comparison between the two diagrams of bifurcation (Figs. 6 and 8), we see that the thresholds for both steady and Hopf bifurcation points have increased when A has been changed from 0 to 40 000, indicating that the convective flows have been stabilized by the acoustic streaming flows.

To have a more detailed information on the stabilization of the convective flow by the acoustic streaming in the three-dimensional cavity, we have followed both bifurcation points by continuation for increasing values of A. The stability diagram giving the evolution of both stationary and Hopf thresholds as a function of the acoustic intensity A for $H_b = 0.62$ is presented in Fig. 10. In the range of the studied values of A, the critical values for both transitions increase monotonously and quite strongly with A. This confirms the clear stabilization effect on buoyant flows which can be obtained by applying acoustic streaming, which in particular allows to delay the onset of oscillatory flows responsible of damages in crystal growth.

4. Conclusion

Our study on the influence of acoustic streaming on the stability of melts flows in horizontal Bridgman configurations has shown that it was possible to stabilize the convective flows by acoustic streaming. For an extended fluid layer submitted to a horizontal temperature gradient, this stabilizing effect can be obtained in the domain of small Prandtl numbers for large acoustic sources with $H_b \geqslant 0.7$. Another way to enhance the stabilization of the convective flow is to decenter the acoustic source, so that the acoustic streaming flow opposes the convective flow. For the more realistic laterally heated three-dimensional

cavity of square cross-section, the stabilization of the convective flows by acoustic streaming has also been shown to be possible. Indeed, for a square acoustic source of characteristic size $H_b = 0.62$, a clear increase of the instability thresholds has been obtained when increasing the acoustic streaming intensity. Finally, our results also indicate that acoustic streaming must be used carefully, as destabilizing effects on the convective flows exist in some parameter ranges.

Acknowledgment

The calculations were carried out on a NEC-SX5 computer with the support of the CNRS through the 'Institut du développement et des ressources en informatique scientifique'.

References

[1] G.N. Kozhemyakin, J. Crystal Growth 149 (1995) 266.
[2] J. Lighthill, J. Sound Vib. 61 (3) (1978) 391.
[3] C. Eckart, Phys. Rev. 73 (1) (1948) 68.
[4] Lord Rayleigh, The Theory of Sound, MacMillan, London, 1929.
[5] W.L. Nyborg, Acoustic streaming, in: M.F. Hamilton, D.T. Blackstock (Eds.), Nonlinear Acoustics, Academic Press, San Diego, 1998, p. 207.
[6] K.D. Frampton, S.E. Martin, K. Minor, Appl. Acoust. 64 (2003) 681.
[7] W. Dridi, D. Henry, H. Ben Hadid, C.R. Mec. 335 (3) (2007) 175.
[8] D. Henry, H. Ben Hadid, Phys. Rev. E 76 (2007) 016314.
[9] C.K. Mamun, L.S. Tuckerman, Phys. Fluids 7 (1995) 80.